Proceedings of the 5th International Symposium on Steel Science (ISSS 2017)
Nov. 13-16, 2017, Kyoto, Japan: The Iron and Steel Institute of Japan

Origin of diffraction profile line broadening of ferrite-cementite steels

Yanxu Wang[1*], Yo Tomota[2], Takahito Ohmura[3], Wu Gong[4], Stefanus Harjo[5]

[1] Kyushu University, 744 Motooka, Nishi-ku, Fukuoka 819-0395, Japan
[2] National Institute for Materials Science, 1-2-1 Sengen, Tsukuba, Ibaraki 305-0047, Japan
[3] National Institute for Materials Science, 1-2-1 Sengen, Tsukuba, Ibaraki 305-0047, Japan
[4] Elements Strategy Initiative for Structural Materials, Kyoto University, Yoshida-honmachi, Sakyo-ku, Kyoto 606-8501, Japan
[5] Japan Atomic Energy Agency, 2-4, Shirane Shirakata, Tokai, Ibaraki 319-1195, Japan

Abstract: Diffraction profile line broadening of ferrite steels containing nearly spherical cementite particles with semi-coherent or incoherent ferrite-cementite interface was studied. Diffraction profile obtained by synchrotron X-ray diffraction shows large line broadening both in ferrite and cementite for the case of the semi-coherent interface. Line broadening during pearlitic transformation and cementite spheroidization annealing was monitored by in-situ neutron diffraction and was found to decrease with cementite speroidization. The interface becomes incoherent by ferrite recrystallization after cold rolling, resulting in drastic decreasing of line broadening to be comparable to that of annealed pure iron.

1. INTRODUCTION

Pearlitic transformation in eutectoid steel has been reported to accompany the volume expansion of 4.76% which brings hydrostatic tensile stresses in austenite and compressive in pearlite [1]. Local internal stresses caused by the misfit transformation strains would be relaxed by plastic deformation near the interface as was suggested by transmission electron microscopy (TEM) observations for a high Mn-C steel in which the untransformed austenite could be kept by interrupted quenching during the pearlitic transformation. In a pearlite colony, either Bagaryatsky [2], Isaichev [3] or Pitch-Petch [4, 5] crystal orientation relationship has been claimed to exist between ferrite and cementite. The ferrite/cementite interface has been reported to be semi-coherent with ledges by TEM observations [6]. Recent electron back-scatter diffraction (EBSD) measurements have revealed that the crystal orientation of ferrite changes even within an individual block, where the cementite orientation also changes along the growing direction of a plate [7]. These recent results indicate the complex internal stresses generated during the pearlitic transformation accompanying some stress relaxation mechanisms. The internal stresses must be added during cooling after transformation because of thermal misfit contraction between ferrite and cementite [8]. Since most previous works were focused on the lamellar structure, those consisting of nearly spherical cementite particles were studied in this paper using neutron and synchrotron X-ray diffractions, scanning electron microscopy (SEM) and EBSD measurements.

2. EXPERIMENTAL PROCEDURES

In the present work, a steel with the chemical composition of Fe-0.8C-0.2Si-0.4Mn (mass pct) made through an industrial process was studied. After patented at 1173 K for 3.6 ks, two kinds of specimens were prepared by different cementite-spheroidization treatments: one was annealing at 973 K for 810 ks followed by furnace cooling (hereafter called specimen A) and the other was cold rolling by 70 pct in reduction followed by annealing at 973 K for 810 ks (specimen B).

The specimens for SEM observations were finished by mechanical polishing and etching with a 5 pct nital and those for EBSD measurements by electrolytic polishing. A field emission gun scanning electron microscope (JEOL JSM-7000F) was used for SEM observations operating at 15 kV. The conditions employed for EBSD measurements were, acceleration voltage: 20 kV, working distance: 15 mm, tilt angle: 70° and step size: 20 nm. The obtained EBSD data were analyzed with the software programs OIM Analysis 7.

Synchrotron X-ray diffraction experiments were performed at BL15XU [9] of SPring-8, operated

* Corresponding author. E-mail: WANG.Yanxu@nims.go.jp, telephone: +81-(0)29-851-3354 EXT3673.

with a high-resolution mode ($\Delta d/d$: ~0.07 pct, where d is d-spacing). The wavelength and diameter of the incident beam were 0.00653 nm and 30 μm, respectively. Disc specimens (10×10×2 mm^3) polished with emery papers were rotated at 60 rpm during measurement for 0.3 ks.

A cylindrical specimen with a diameter of 8 mm and a length of 30 mm was prepared for in-situ neutron diffraction experiments during pearlitic transformation and cementite spheroidization annealing using a high-resolution time-of-flight (TOF) neutron diffractometer for engineering materials sciences (BL19, TAKUMI) at the Materials and Life Science Experimental Facility (MLF) of the Japan Proton Accelerator Research Complex (J-PARC). A thermocouple was welded onto the specimen surface to measure and control temperature. The specimen was heated in vacuum with a heating rate of 0.5 K/s, austenitized at 1173 K for 1.2 ks, and then held at 873 K for 5.4 ks. Subsequently, the specimen was heated up to 973 K for cementite spheroidization for 30.7 ks. Ex-situ neutron diffraction measurements were also carried out for specimens with 10×10×10 mm^3.

3. RESULTS AND DISCUSSION

3.1. Microstructures

Figure 1 show SEM micrographs of specimens A and B. As can be observed, cementite particles are dispersed in the coarse-grained ferrite matrix (grain size: approximately 24 μm) in specimen A (a), whereas in fine-grained (4 μm) in specimen B (b).

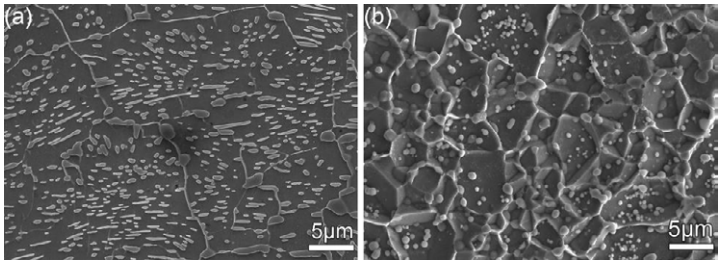

Fig. 1 SEM micrographs of specimen A (a) and B (b).

3.2. Features of inverse pole figure (IPF) maps obtained by EBSD

EBSD results for specimens A and B are exhibited in Fig. 2. Here, the IPF and image quality (IQ) maps were combined to identify constituent phases. Gradient distribution of ferrite crystal orientation is found within individual ferrite grains in specimen A (a) but not in B (b). Such an orientation graduation was reported in lamellar pearlite steels [10]. It is made clear that the orientation graduation remains even after the shape change of cementite particles and that it disappears after the recrystallization of ferrite (see Fig. 2(b)). More details will be reported elsewhere together with the case of lamellar pearlite structure.

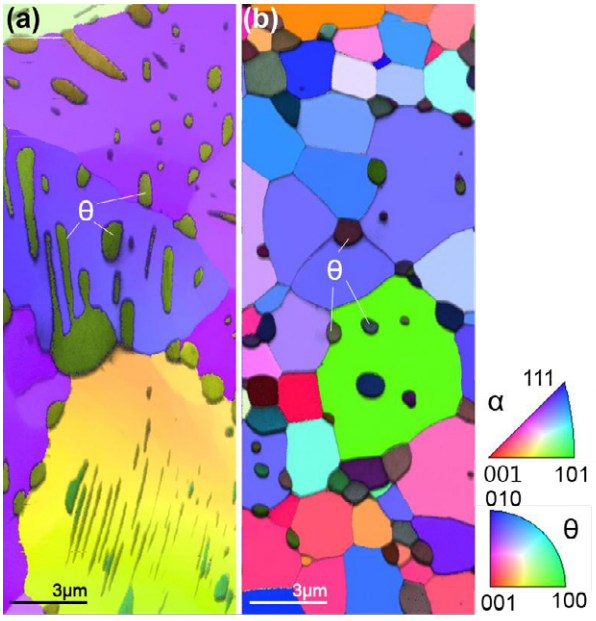

Fig. 2 Combined IQ and IPF maps: (a) specimen A and (b) B.

3.3. Diffraction profiles obtained by ex-situ synchrotron X-ray and neutron diffractions

Figure 3(a) displays line profiles obtained by ex-situ synchrotron X-ray diffraction for specimens A and B. The diffraction intensity was plotted by log-scale for the vertical axis to show low-intensity diffraction peaks from 14 vol. pct fraction of cementite (orthorhombic structure) and line broadening near the background clearly. The difference in line broadening between specimens A and B can be apparently recognized. The detailed comparison on line broadening is presented in Fig. 3(b) for ferrite 110 and (c) for cementite 112 by normalizing peak intensities and positions. Notably, not only the ferrite peak but also the cementite peak exhibits a large line broadening in specimen A, indicating that the internal stresses are balanced between the two phases. A similar trend can be confirmed in Fig. 3(d) of the results by ex-situ neutron diffraction. Since the resolution of neutron diffraction of this experiment is ~0.3 pct, the difference between specimens A and B is small. It is, however, important to check the local information obtained near the surface with the global information obtained from a bulk specimen

by neutron diffraction, because these two results are, in some cases, different from each other. Additionally, the line profile obtained from pure iron was drawn in Fig. 3(d), showing the quite small difference with that of specimen B. It suggests that the internal stresses generated by pearlitic transformation were completely relaxed by ferrite recrystallization. According to the recent HRTEM observations [11], the ferrite/cementite interface of specimen A is semi-coherent. The ferrite recrystallization is believed to change the interface character to incoherent, resulting in a decrease of internal stress, i.e., FWHM. It must be interesting that that specimen A presents continuous yielding behavior whereas specimen B discontinuous. According to the nano-indentation examinations, the pop-in load is smaller near the interface of specimen A compared with the inside of grain or near the interface of specimen B. As will be tabulated later (Table 1), these results suggest that the dislocation emission seems to take place more easily at or near the semi-coherent interface with ledges of specimen A.

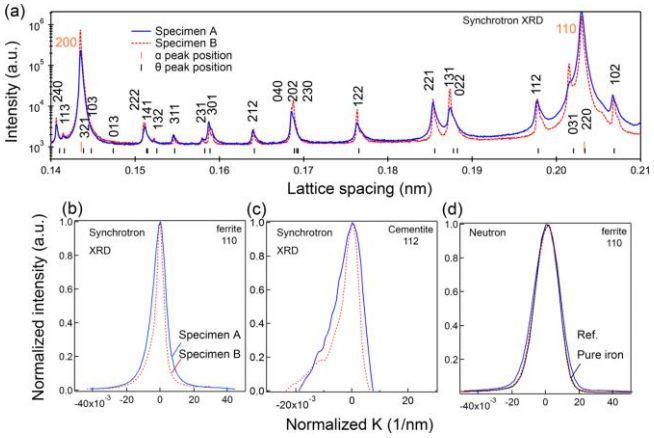

Fig. 3 Features of diffraction profiles: (a) whole profiles obtained by synchrotron X-ray diffraction for specimens A and B, (b) normalized ferrite 110 profiles, (c) normalized cementite 112 and (d) normalized neutron diffraction profiles of 110 ferrite including pure iron. Here, $K=1/d$; d is d-spacing (nm).

3.4. Results of in-situ neutron diffraction measurements

To obtain further insights on the origin of diffraction line broadening, in-situ neutron diffraction measurement was performed during pearlitic transformation and cementite spheroidization behavior.

Figure 4 is the summary of this experiment in which a temperature history employed is presented in (a). Change in diffraction profiles during the experiment is shown in (b) as two-dimensional change focusing on ferrite 110 and austenite 111 peaks. As seen, austenite 111 peak appears by heating up to 1173 K to be a single austenite state in the beginning and then disappears with isothermal holding at 873 K. On the other hand, ferrite 110 peak disappears during heating to 1173 K and appears at subsequent

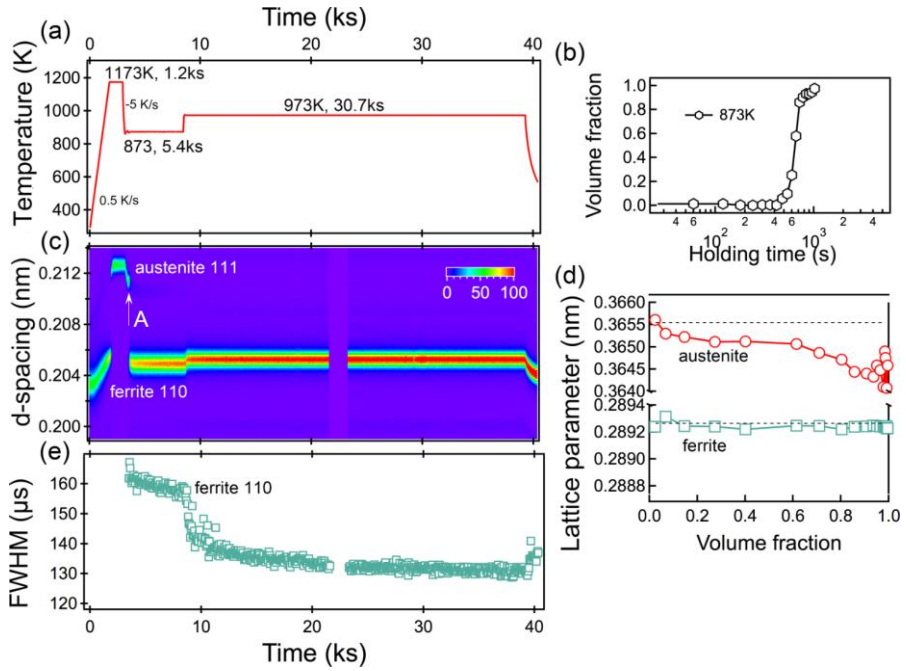

Fig. 4 Results of in-situ neutron diffraction during pearlitic transformation: (a) heat-treatment schedule, (b) change in pearlite volume fraction with holding time at 873 K, (c) two-dimensional profiles for 110 α and 111γ peaks during the test, (d) changes in lattice parameter of austenite and ferrite with holding time at 873 K and (e) change in FWHM of ferrite 110 peak with time with experimental time.

873 K holding. Here, large peak shifts are observed related to reheating to 973 K and cooling at the end and neutron beam was stopped in a short time during 973 K holding. An arrow labeled "A" indicate the finish of pearlitic transformation. The obtained neutron diffraction profiles were analyzed using the Z-Rietveld software [12]. Fig.4 (d) shows the change in volume fraction of pearlite during isothermal holding at 873 K, indicating that pearlitic transformation was completed within 0.6 ks. The change in lattice parameters for austenite and ferrite are plotted in Fig. 4(e). Note that the lattice parameter of austenite is found to decrease after the onset of pearlitic transformation, while that of ferrite is almost constant. The lattice parameter of austenite would be predicted to increase because pearlitic transformation accompanies volume expansion [1]. Hence, the decrease in lattice parameter of austenite is puzzling and likely caused by decreasing of carbon concentration in the untransformed austenite. During the isothermal holding, full width at a half maximum (FWHM) in ferrite 110 peak is found to decrease as shown in Fig. 4(c), probably due to the shape change of cementite particle. That is, the decrease in ferrite/cementite interface area per unit volume would result in decreasing of FWHM. It is also found that FWHM increases a little upon the final cooling. It may be related to thermal misfit strains.

4. SUMMARY

The comparison of the two specimens would be summarized as shown in Table 1. The difference is believed to stem from the pearlitic transformation character. The recrystallization of plastically deformed ferrite seems to change the interface character from semi-coherent to incoherent, resulting in a drastic decrease of internal stresses which are mainly corresponding to the magnitude of FWHM of diffraction profiles.

Table 1 Comparison of characteristic features of specimens A and B

Specimen	Shape of cementite	Ferrite grain size	Crystal orientation within a block	OR between ferrite and cementite	Interface character	Yielding behavior*	Yielding after strain aging*
A	near spherical	24 μm	change	close to Bagaryatsky	Semi-coherent	continuous	almost continuous
B	spherical	4 μm	not change	no specific OR	incoherent	dis-continuous	dis-continuous

*not included in this paper but will be reported elsewhere.

Acknowledgements: The authors are grateful to Dr. M.Tanaka of NIMS synchrotron X-ray station at SPring-8 for the support of the X-ray diffraction measurements (#2015B4502). Neutron diffraction measurements were performed through the project #2015A0153.

REFERENCES

[1] A. Durgaprasad, S. Giri, S. Lenka, S. Kundu, S. Mishra, S. Chandra, R.D. Doherty, I. Samajdar, Acta Mater., 129 (2017) 278-289.
[2] Y.A. Bagaryatsky, Dokl. Akad. Nauk. SSSR, 73 (1950) 1161-1164.
[3] I.V. Isaichev, Zh. Tekh. Fiz., 17 (1947) 835-838.
[4] N.J. Petch, Acta Cryst., 6 (1953) 96.
[5] W. Pitsch, Acta Metall., 10 (1962) 79-80.
[6] D.S. Zhou, G.J. Shiflet, Metall. Trans. A, 23A (1992) 1259-1269.
[7] N. Nakada, N. Koga, T. Tsuchiyama, S. Takaki, Scripta Mater., 61 (2009) 133-136.
[8] I.G. Wood, L. Vočadlo, K.S. Knight, D.P. Dobson, W.G. Marshall, G.D. Price, J. Brodholt, J, Appl. Crystallogr., 37 (2004) 82-90.
[9] M. Tanaka, Y. Katsuya, Y. Matsushita, O. Sakata, J. Ceram. Soc. Jpn,, 121 (2013) 287-290.
[10] N. Koga, N. Nakada, T. Tsuchiyama, S. Takaki, M. Ojima, Y. Adachi, Scripta Mater., 67 (2012) 400-403.
[11] Y. Wang, Y. Tomota, T. Ohmura, CAMP-ISIJ, 30 (2017) 868.
[12] R. Oishi, M. Yonemura, Y. Nishimaki, S. Torii, A. Hoshikawa, T. Ishigaki, T. Morishima, K. Mori, T. Kamiyama, Nucl. Instruments and Methods Phys. Sect. A, 600 (2009) 94-96.